Adaptive Optics Facility. When cutting-edge technology meets operational robustness and performance

P.-y Madec

Adaptive Optics Facility
When cutting-edge technology meets operational robustness and performance

P.-Y. Madec, on the behalf of the AOF team

European Southern Observatory, Karl Schwarzschild Str 2, D-85748 Garching

ABSTRACT

The Adaptive Optics Facility (AOF) is an ESO project started in 2005, which transformed Yepun, one of the four 8m telescopes in Paranal, into an adaptive telescope. This has been done by replacing the conventional secondary mirror of Yepun by a 1172 actuator Deformable Secondary Mirror (DSM) and attaching four Laser Guide Star (LGS) Units to its centerpiece, each of them featuring a high stability narrow-band 20 W laser. Additionally, two Adaptive Optics (AO) modules (GALACSI serving MUSE a 3D spectrograph, and GRAAL, serving Hawk I a wide field infrared imager) have been assembled onto the telescope Nasmyth adapters, each of them incorporating four LGS WaveFront Sensors (WFS) and one tip-tilt sensor used to control the DSM at 1 kHz frame rate. These WFSs are based on 0 Read-out Noise (RoN) detectors. The complete AOF has been operated on-sky for more than 2 years and is routinely delivering science.

This paper presents the most important and amazing features of the AOF, focusing on cutting-edge technology in use, operational concept and overall performance. In the first part of the paper, the AOF design is recalled, with a focus on the DSM, the lasers, the WFS cameras and the Real Time Computer technology. Then, the acquisition sequence and overall on-sky operation efficiency will be detailed; finally, on-sky performance of AOF will be presented.

Keywords: Adaptive Optics – Ground Layer Adaptive Optics – Laser Tomography Adaptive Optics – Adaptive Optics on-sky operation – Deformable Secondary Mirror – Laser Guide Star

1. INTRODUCTION

The Adaptive Optics Facility (AOF) is an ESO project started in 2005 [1], which transformed Yepun, the 8m Unit Telescope 4 (UT4) in Paranal, into an adaptive telescope. This has been done by replacing the conventional secondary mirror of Yepun by a Deformable Secondary Mirror (DSM) and attaching four Laser Guide Star (LGS) Units to its centerpiece. Additionally, two Adaptive Optics (AO) modules (GALACSI serving MUSE a 3D spectrograph, and GRAAL, serving Hawk I a wide field infrared imager) have been assembled onto the telescope Nasmyth adapters, each of them incorporating four LGS WaveFront Sensors (WFS) and one tip-tilt sensor used to control the DSM at 1 kHz frame rate.

Following a 10-years design, technological development, integration and test phase in Europe [2] [3], AOF started to be assembled on Yepun in 2015. First, GRAAL [4] and the LGS Unit (LGSU) #1 have been installed on the telescope and tested together; while the DSM was not yet available. Following this successful first step, the 4 Laser Guide Star Facility (4LGSF) installation has been completed beginning of 2016, the first light obtained in April 2016 and the full commissioning completed mid 2016 [5]: all specifications were met especially the return flux (larger than 8 10^6 photons/m^2/s), the LGS spot size (1.35 arcsec fwhm under good seeing conditions) and the pointing accuracy (better than +/- 2.5 arcsec on-sky). Mid-October 2016, Yepun has been closed for two months. The old Dornier M2 Unit has been removed and the new DSM installed [6] [7]. First light has been possible within few days following the installation: the DSM was operated in non-AO mode and all functionalities of the Dornier M2 were available. It took then few weeks to fully recommission the telescope (tracking, guiding, field stabilization, chopping, focus and coma correction), and its associated four foci/instruments (SINFONI, HAWK-I, MUSE and the VLTI). The telescope has been returned to science mid of December and since then is used in normal operation. In March 2017, GALACSI has been installed on Yepun [6]. The first light of MUSE/GALACSI Wide Field Mode (WFM) has been reached in June [8] and the Science Verification (last step of the commissioning) completed in August [9]. Since October 2017, MUSE/GALACSI WFM has been used in

normal operation, delivering science to the community. In December 2017, HAWK-I/GRAAL obtained its first light, followed by a successful Science Verification in January 2018. Finally, MUSE/GALACSI Narrow Field Mode (NFM) got first light in June 2018, and its Science Verification happened in September 2018.

AOF commissioning is now complete, and the astronomical community is benefitting from the fantastic performance of this facility for more than 2 years.

In section 2, the main features of the most critical AOF components are described: section 2.1 is dealing with the DSM, section 2.2 with the 4LGSF, section 2.3 with the WFS cameras and section 2.4 with SPARTA, the AOF Real Time Computer (RTC). Section 3 details the AOF acquisition and observation sequence on-sky, and finally section 4 illustrates the unprecedented capabilities of the AOF by presenting typical results obtained with the Laser Tomography AO (LTAO) mode of MUSE.

2. AOF AT THE FOREFRONT OF THE TECHNOLOGY

2.1 The Deformable Secondary Mirror

The DSM has been manufactured by Microgate and ADS, two Italian companies. It is based on the use of a thin optical shell (1.12 m diameter – 2 mm thick – manufactured by SAGEM-REOSC – see Figure 1, top-right) associated to voice coil actuators. On the back of the shell, 1172 magnets are glued, facing 1172 voice coils actuators. One capacitive sensor is associated to each and any actuator, each of them measuring the distance between the thin shell and a reference body. This reference body is one of the core components of the DSM, as it defines the stability of the optical surface with temperature and gravity; it is a highly light-weighted piece of optics, made out of Zerodur; it has been manufactured by SESO (see Figure 1, left).

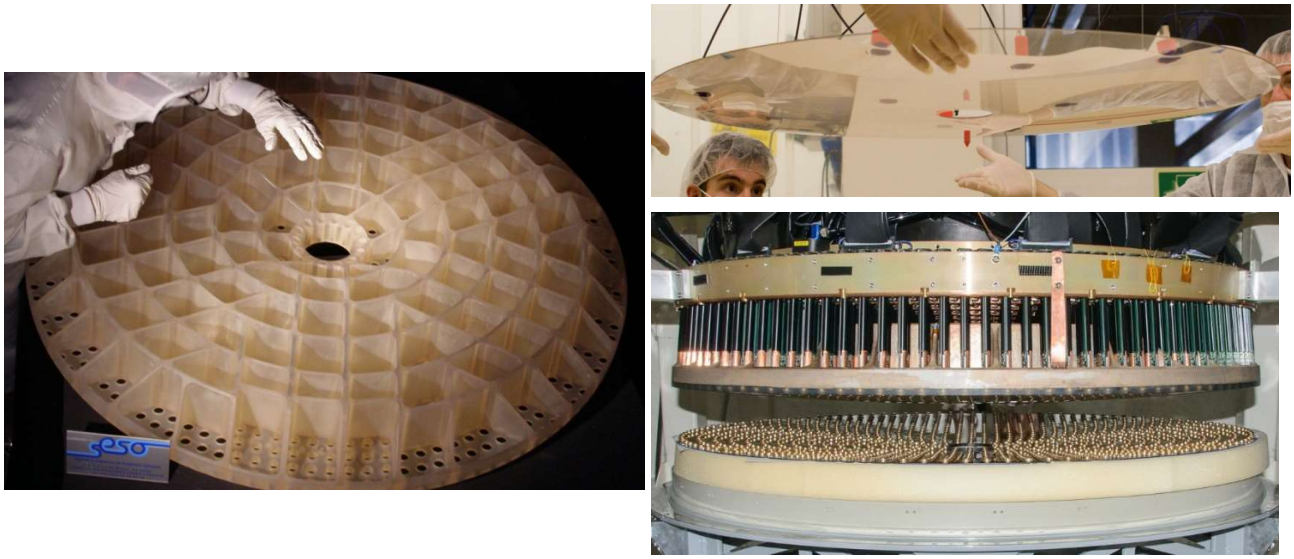

Figure 1 – Left: reference body as seen from the back; 1.1 m diameter; Zerodur; less than 40 kg; manufactured by SESO – Top right: optical thin shell; 1.1 m diameter; 2 mm thick; manufactured by REOSC – bottom right: the complete optical head, during its final integration phase; on the top 1172 coils attached to the cold plate (aluminum) and going through the reference body; on the bottom, the thin shell with 1172 permanent magnets glued on the rear face; assembled by ADS and Microgate

A local servo loop running at 70 kHz locks the actual distance measured by the sensors to a reference position defined by the customer (either GRAAL or GALACSI), by controlling the current injected in the coils. The reference position (vector of DSM commands) can be updated at 1 kHz; the DSM reaches its position with a settling time of 0.7 ms (see Figure 2, right). The best optical flat at rest of the DSM can be as low as 18 nm rms wavefront error [10] (see Figure 2, left). The stroke of the DSM is equal to +/- 35 microns for low order modes, and is limited by the maximum force the voice coils can generate (+/- 1 N) for high order modes. The maximum tip-tilt stroke on sky is +/- 5.5 arcsec.

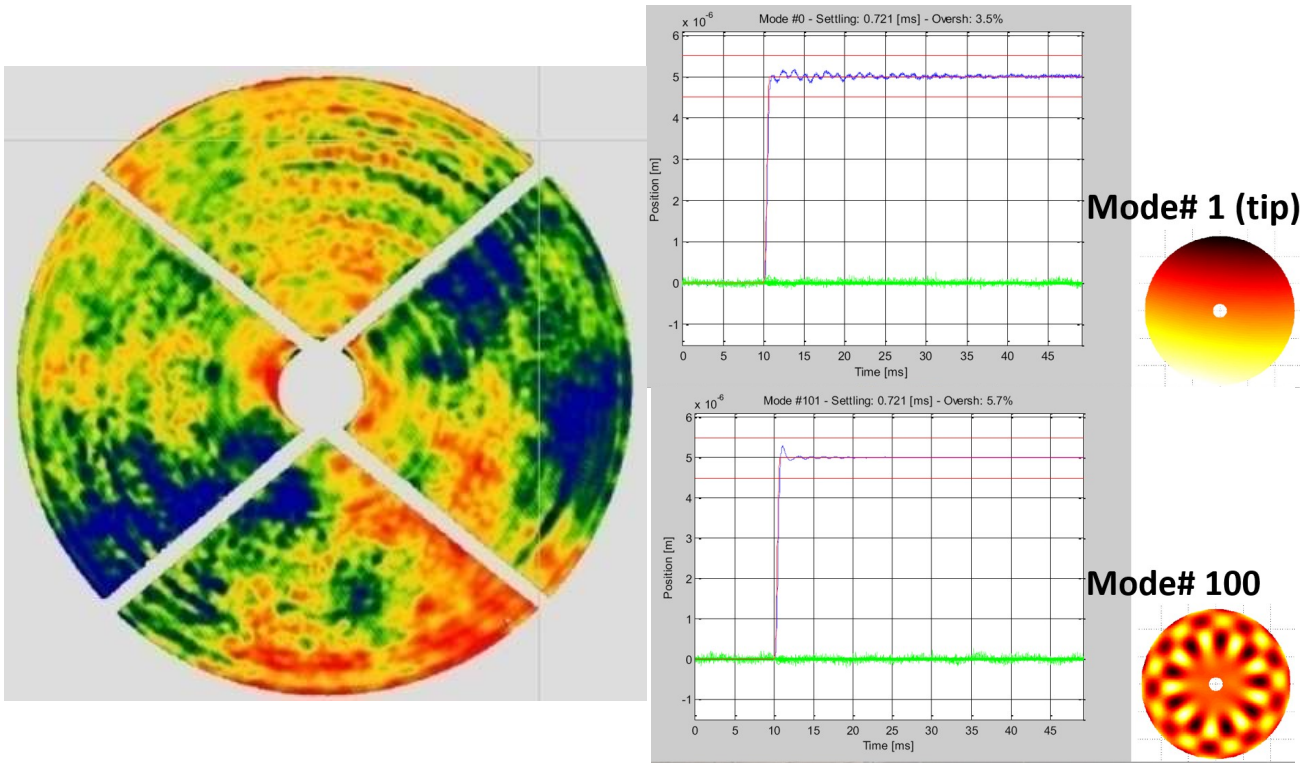

Figure 2 – Left: interferogram of the DSM best flat; 18 nm rms wavefront error; rings are coming from one of the mirrors of the test tower – Right: DSM step response, for the modes 1 (tip) and 100; the settling is as short as 0.7 ms for both modes, with a very good damping.

2.2 The 4 Laser Guide Star Facility

The 4LGSF is made of 4 identical LGSUs, each one featuring a 20+2 W cw fiber laser and a launch telescope. The 4 lasers have been manufactured by Toptica (Germany) and MPBC (Canada); they are based on a Master Oscillator / Power Amplifier (MOPA) approach. The master laser is an ultra-stable laser diode emitting few mW of light at 1178 nm (the line bandwidth is as narrow as 5 MHz). It is injected in a monomode polarization maintaining fiber coil, and is Raman amplified with the help of a 100 W pump fiber laser operating at 1120 nm, itself pumped by a set of high power laser diodes. At the output of the Raman amplifier fiber, 36 W of ultrastable linearly polarized laser light at 1178 nm is available, injected in a doubling frequency cavity and converted into 22 W of 589 nm laser light. The optical quality of the beam is better than 15 nm rms.

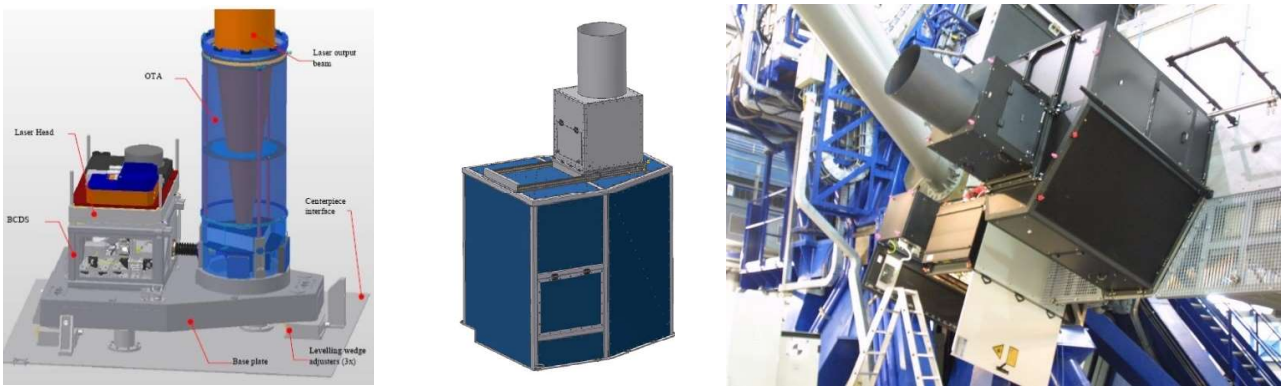

Figure 3 – Left: CAD view of one LGSU showing the launch telescope and the laser head on top of the BCDS – Center: CAD view of the wind baffle, protecting the LGSU once on the telescope – Right: picture of one LGSU installed on Yepun's Center Piece

Each laser head is sitting on top of a Beam Control and Diagnostic System (BCDS) featuring a Beam Expander Unit made of a small magnifier used to adjust the focalization of the laser to the Na layer, and a fast tip-tilt mirror to correct the uplink and down link laser jitter; the beam is then expanded by a 40 cm diameter refractive launch telescope, and propagated to the sky as a 22 cm e^{-2}-diameter gaussian beam (see Figure 3). Each launch telescope is equipped with a quarter waveplate to deliver a circularly polarized beam and with a slow steering mirror to position each LGS at its predefined position (from 0 to 6 arcmin from the Yepun optical axis.

The return flux coming from each LGS is consistently varying from 8 to 20 10^6 photons/m^2/s depending on its position on sky (see Figure 4). The spot size has been measured to be 1.35 arcsec under good seeing conditions. The pointing accuracy of each LGSU is +/- 2.5 arcsec on-sky [5].

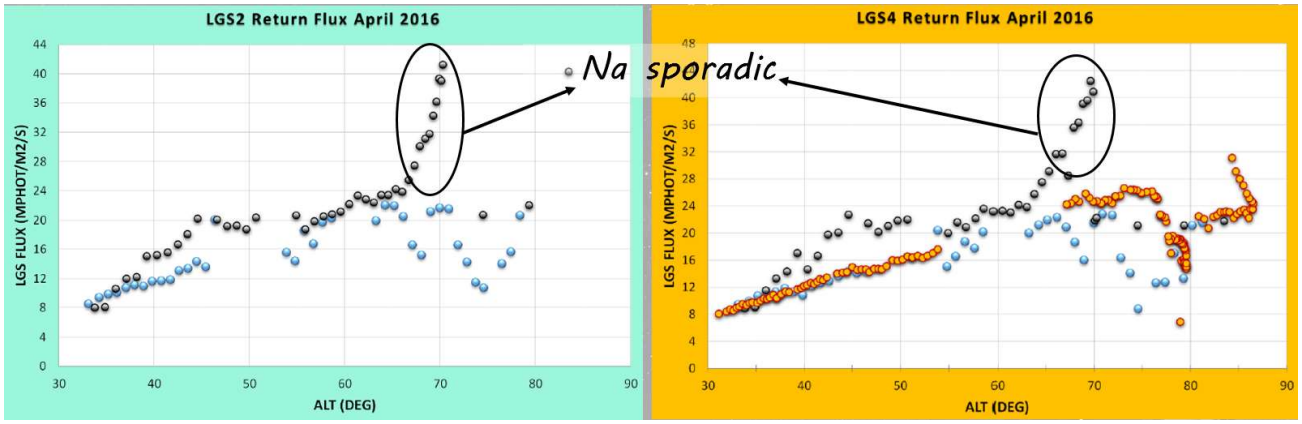

Figure 4 – Laser return flux as a function of the telescope altitude angle (90 degrees is zenith), measured on-sky during the 4LGSF commissioning in April 2016 – the different colors correspond to different nights – during one night, a Na sporadic was experienced, bringing a factor of 2 improvement in the return flux (40 10^6 photons/m^2/s)

2.3 The 0 Read-out-Noise Cameras

ESO and JRA2 "Fast Detectors for Adaptive Optics" FP6 OPTICON network funded e2v to develop a compact Peltier cooled sensor, the CCD220, to meet the requirements of WFSs for the 2nd Generation of VLT instruments (SPHERE, AOF – MUSE and HAWK-I).

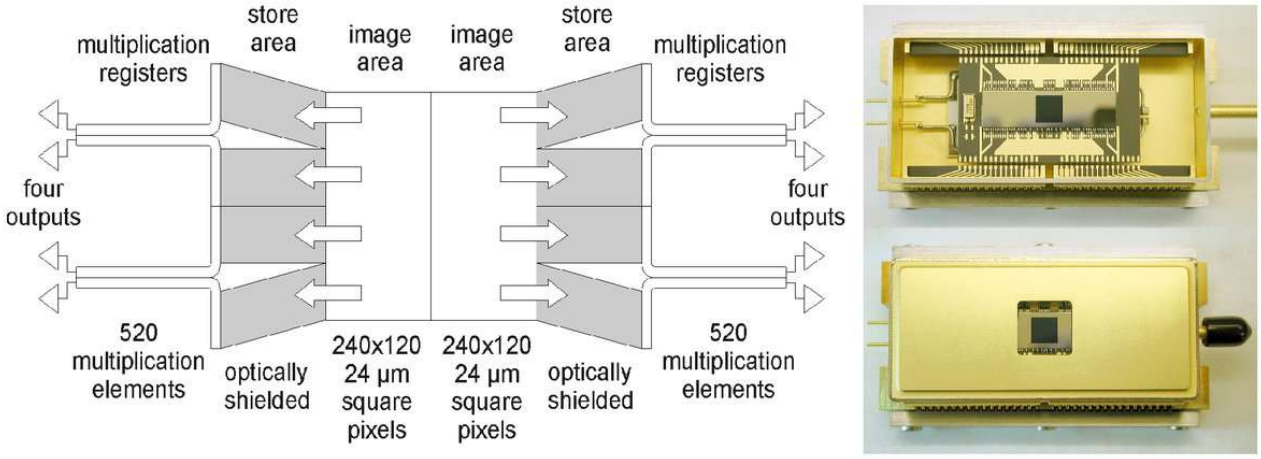

Figure 5 - Left: Schematic of e2v 240x240 pixel L3Vision CCD220. Eight electron-multiplying (gain) registers enable sub electron noise at frame rates of > 2000 fps – Right: Photograph of CCD220 package. The package contains an integral Peltier that cools the CCD below -45°C to achieve < 0.05 e-/pix/frame total dark current at 100fps.

The CCD220 (schematic left in Figure 5) is a 24 µm square 240x240 pixels split frame transfer back illuminated L3Vision CCD. Eight electron-multiplying gain L3Vision registers operating at greater than 20 Mpixel/s enable sub electron noise

to be achieved at frame rates in excess of 2000 fps. With an output amplifier read noise of 65e^- at unity gain, a modest electron-multiplying gain of 650 results in an overall effective read noise of under 0.1 e^-.

The CCD220 is encapsulated in a 64-pin package (right in Figure 5) with a custom-designed integral Peltier cooler that cools the CCD below -45°C to achieve dark currents < 0.05 e^-/pix/frame. Table 1 contains a summary of the main performance parameters of the CCD220 [11]. For applications that require high QE in the "red" (700-950nm), the CCD220 is available in Deep Depletion silicon (CCD220-DD). The CCD220-DD has > 75% higher QE in the "red" than the standard silicon device and is used for SPHERE and the AOF tip-tilt sensors.

Requirement	Measurements
Frame Rate (fps)	> 1500
Read noise at gain of 1000 and 1500fps	< 0.1e-
Image Area Full Well (e-)	> 160k
Serial Charge Transfer Efficiency	0.99999
Cosmetic (number of traps, bright, and dark defects)	0
Dark Current at 1200fps and -40°C (e-/pixel/frame)	< 0.02
Dark Current at 100fps and -45°C (e-/pixel/frame)	< 0.05

Table 1 - Performance of e2v CCD220-DD routinely met with AONGC cameras.

The CCD220s together with the ESO NGCs (New General Controllers) are assembled in mechanical frames providing cooling and power (see Figure 6).

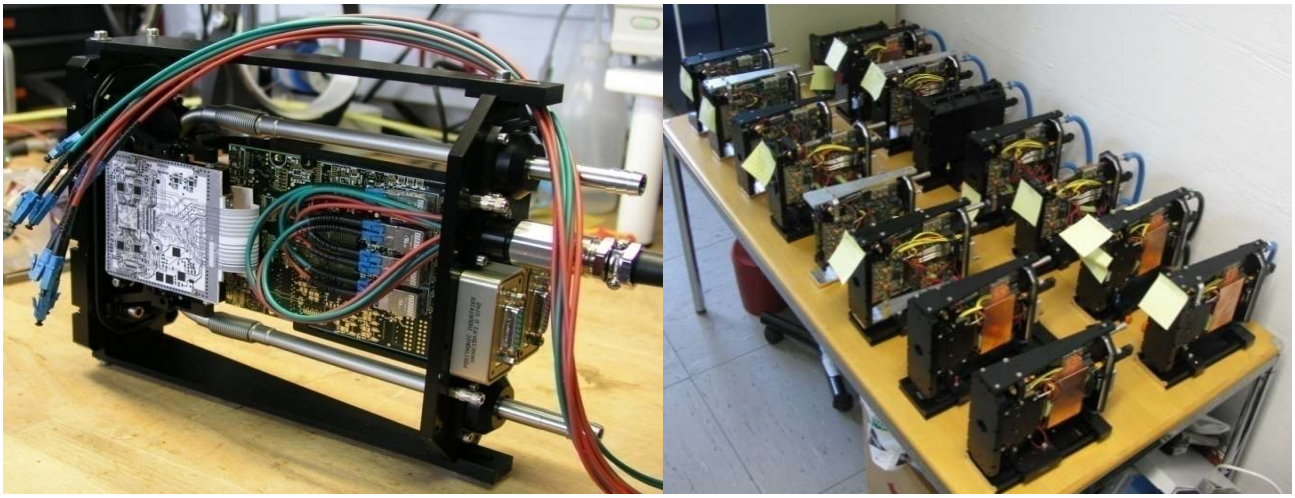

Figure 6 – Left: mechanical housing of the AOF WFS cameras, including front end electronics, cooling and power – Right: the 16 AOF WFS cameras, before their final integration

2.4 SPARTA, the AOF Real-Time Computer

SPARTA, the ESO Standard Platform for Adaptive optics Real Time Applications [12], is the high-performance, real-time computing platform serving four major instruments at the VLT: SPHERE, GALACSI/MUSE, GRAAL/HAWK-I and ERIS.

The two main component blocks of a SPARTA RTC are shown in Figure 7: the low-latency RTC Box, and the Co-Processing Cluster used to perform on-line optimization and AO loop supervision.

The RTC Box encapsulates a hard real-time, low-latency processing pipeline which implements all the operations required at the loop rate in order to close the inner AO loops. This involves first the Wavefront Processing -i.e. computation of local wavefront gradients from WFS pixel frames, then the Reconstruction -i.e. computation of delta actuator commands from

local WFS gradients and finally the Control –i.e. time filtering of delta actuator commands, typically involving IIR (Infinite Impulse Response) control (at least integral) plus some form of saturation management.

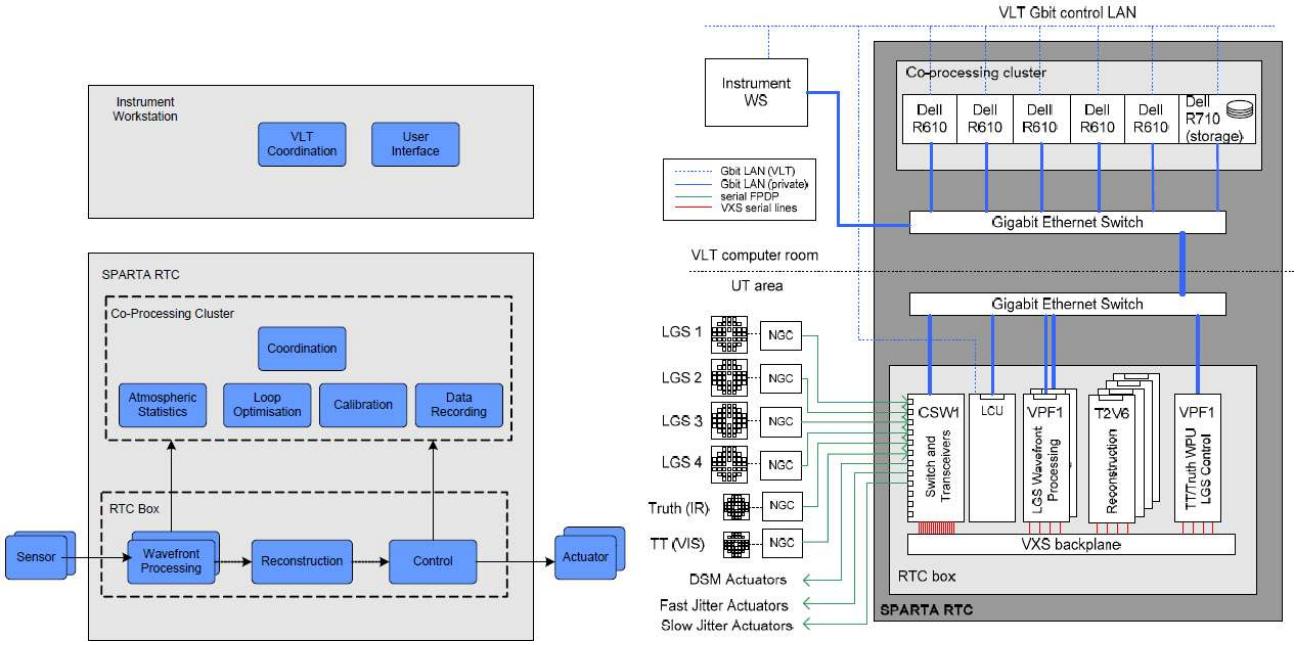

Figure 7 – Left: main component blocks and AO real-time pipeline processing stages in a SPARTA RTC – Right: example of hardware deployment of a SPARTA RTC for an AOF-like configuration

The Co-processing Cluster based on multi-CPU, multi-core Linux computers continuously receives loop telemetry data from the RTC Box (e.g. local wavefront gradients and actuator commands at loop rate) and further processes them to implement soft real-time computations requested by the secondary AO loops' closure (e.g. RTC Box parameters optimization, offloading to external actuators, etc.) as well as auxiliary tasks such as atmospheric statistics, or AO loop performance monitoring.

As a performance metrics, one very often uses the so-called RTC latency. This latency is defined as the time elapsed from the availability of the last pixel of the WFS camera to the application of the DSM commands. The RTC latency is one important term in the overall AO loop latency budget driving the temporal performance of the AO system: the smaller the latency, the higher the rejection cut-off frequency of the AO loop, and the better the turbulence correction. The latency of the AOF SPARTA RTC Box has been measured to be as small as 80 µs (see Figure 8).

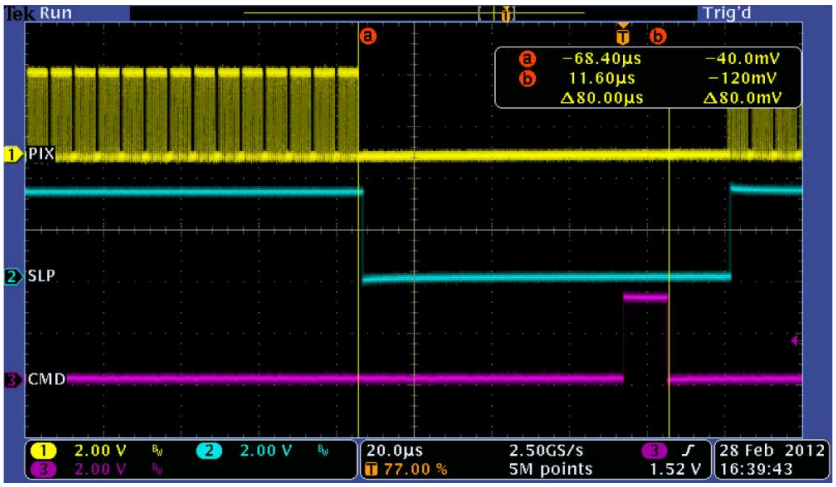

Figure 8 - Oscilloscope plot of an end-to-end SPARTA RTC Box latency measurement. Cursor **a** marks the last pixel (PIX channel) received by the RTC Box, whereas cursor **b** marks the last command (CMD channel) sent 80µs later.

3. AOF ON-SKY OPERATION

Together with the development and the installation of the DSM and the 4LGSF on Yepun, the AOF project also covered the design, manufacturing, test and commissioning of two AO WFS modules: GRAAL and GALACSI.

GRAAL is serving HAWK-I, a 7x7 arcmin^2 IR imager, and provides a Ground Layer Adaptive Optics (GLAO) correction in the full field of view of the instrument. GRAAL is making use of 4 LGS WFS and one visible Tip-Tilt Sensor (TTS). The 4 LGSs are located 6 arcmin from the optical axis of the telescope, allowing to completely free the scientific field of view of HAWK-I.

GALACSI is serving MUSE, a visible 3D spectrograph. MUSE is featuring two modes: a Wide Field Mode with a 1x1 arcmin^2 field of view, and a Narrow Field Mode with 7.5x7.5 arcsec^2 field of view. In WFM, GALACSI delivers a GLAO correction within the MUSE field of view, while in NFM GALACSI must provide MUSE with diffraction limited images thanks to Laser Tomography Adaptive Optics. In its WFM, GALACSI is making use of 4 LGSs located at 64 arcsec from the telescope optical axis and one visible Tip-Tilt star. In its NFM, GALACSI is also using 4 LGSs but located much closer to the telescope axis (10 arcsec). The IR light of the science object is used to feed an IR Low Order Sensor (IRLOS) delivering tip-tilt and focus measurements. The measurements coming from the 4 LGS WFS are combined through a tomographic algorithm to reconstruct the turbulent volume above the telescope. Atmospheric aberrations are then projected on the DSM looking towards the center of the telescope field of view [13] [14].

Operating a science instrument together with a GLAO system makes only sense if the gain in integration time brought by the AO correction is not reduced by the time required to set the complete system. Therefore, besides the image quality performance, one important AOF requirement is to constrain overheads (LGS and NGS acquisition, AO parameter setting, loops closure, etc…) to less than 2 minutes.

During the design, integration and test of the AOF, most efforts have been focused on reaching this goal. In terms of design, both the 4LGSF and the DSM have been specified to be robust and turn-key systems. Microgate/ADS on the one hand and Toptica/MPBC on the other hand have been spending time, effort and creativity to meet this important goal, and the on-sky operation has demonstrated so far that their efforts paid-off. The ESO Laser Group developed and integrated the LGSUs with the same goal in mind: they delivered a system which mechanical stability and internal control allow to reach a positioning accuracy on-sky better than the field of view of the AOF WFSs, reducing dramatically the overall AOF overheads. The mechanical and integration engineers of ESO designed both GRAAL and GALACSI to be stiff enough to avoid uncontrolled drifts and differential flexures of their internal components. Last but not least, the ESO SW engineers have been working in close collaboration with the AOF system and commissioning engineers to parallelize most of the AOF acquisition tasks and to make use of the time required by the telescope to slew and set its active optics, to run all AOF and instrument preset and bootstrap steps [15] [16].

The AOF acquisition sequence is presented in Figure 9. Most of the steps are described for the MUSE WFM acquisition sequence. The GRAAL/HAWK-I and the MUSE NFM acquisition sequences differ only marginally from the MUSE WFM one. These steps are described hereafter:

- Preset phase: during this phase, the telescope, MUSE, the 4LGSF and GALACSI are preset in parallel. The telescope slews to the position of the MUSE science target. All MUSE actuators are set, and calibration images are recorded. The 4LGSF positions the 4 LGSs to their nominal on-sky position and enables all required tracking loops (focusing and tracking). GALACSI actuators are set to their WFM position, all WFS camera gains are set to 1 (safe mode of the cameras avoiding any over-illumination during the telescope slewing) and SPARTA is deployed in its WFM configuration
- Tip-Tilt Sensor bootstrap: when the preset phase is completed (the telescope is tracking and the field stabilization is on), the tip-tilt sensor camera gain is set to its nominal value, which depends on the brightness of the reference source, the NGS is detected and centered in the tip-tilt sensor field of view and the tip-tilt sensor field selector tracking is enabled, based on sidereal trajectography.
- LGS acquisition: once the tip-tilt sensor bootstrap is completed, SPARTA takes control of the 4LGSUs. Based on an internal pointing model built from the 4LGSF one to which the internal GALACSI flexures have been added, the 4 LGSs are positioned on sky. If required (some mechanical hysteresis cannot be calibrated out in the pointing model), a spiral search is started to fine center the 4 LGSs in the GALACSI WFSs; the spiral is applied by making use of the 4LGSF jitter mirrors. It takes less than 10 seconds to find all LGSs and to lock them (jitter loop closure) into the WFSs'

field of view. This critical step of the 4LGSF acquisition sequence has demonstrated to be very robust (almost 0 failure) and fast.

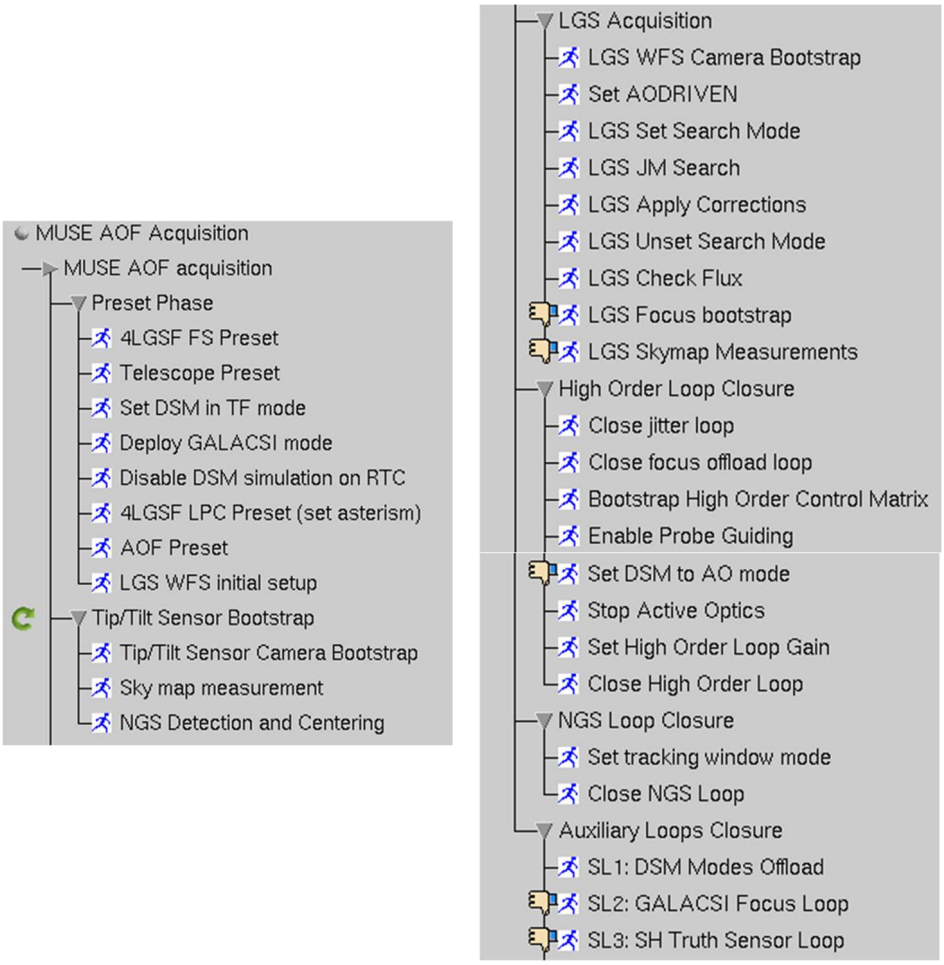

Figure 9: AOF acquisition sequence

- High Order Loop closure: once the 4 LGSs are acquired and locked in position, the high order loop can be closed. The DSM is first set in real-time mode (it accepts commands from SPARTA); then the high order control matrices are loaded into SPARTA, depending on the telescope elevation (management of the mis-registration between the DSM and the GALACSI WFSs). The high order loop can then be closed and the telescope active optics disabled (to avoid a competition between these two loops).
- NGS loop closure: once the high order loop is closed, the tip-tilt loop can then be closed safely; this step is very fast and takes only a couple of seconds.
- Auxiliary loop closure: once all fast loops are locked, the auxiliary loops can then be closed. They are taking care of the telescope active optics (offload of the DSM low order modes onto M1), and of managing the GALACSI focus, mis-registrations with the DSM, camera background, weighting maps update, etc…

At this stage of the acquisition sequence, the observation with MUSE can start.

The overheads due to the AOF have been measured on-sky during the commissioning nights: it never exceeds 2 minutes and the overall sequence has shown to be very robust. Only one operator is requested to operate the complete system, despite its complexity. This achievement is one of the great success of the AOF. It paves the way for the ELT instruments operation.

4. AOF LASER TOMOGRAPHY AO PERFORMANCE

During the first semester of 2018, GALACSI and MUSE NFM have been commissioned together. On-sky data have been collected to evaluate the performance of GALACSI NFM, defined as the delivered Strehl Ratio at 650 nm. The results obtained on-sky are detailed in [14]. In a nutshell, the LTAO of GALACSI can deliver a Strehl Ratio at 650 nm better than 5% for seeing values up to 0.8 arcsec and a maximum NGS magnitude of 14. This corresponds to image quality of 30 mas. In very good seeing conditions (better than 0.5 arcsec), GALACSI LTAO delivers Strehl Ratio larger than 10% at 650 nm, with fwhm better than 20 mas. This performance is illustrated in Figure 10 where the image of NGC 6388 observed with MUSE and GALACSI is presented. On the left, the image corresponds to a WFM observation (GLAO mode), within a 1arcmin x 1arcmin field of view; the image quality is 0.4 arcsec fwhm. The image in the middle corresponds to the central part of the GLAO image: the field of view is 7arcsec x 7arcsec and the image quality is still 0.4 arcsec. On the right, the image corresponds to the same area as the image in the middle, but when the LTAO is enabled: the field of view is again 7arcsec x 7arcsec, but the image quality is now better than 0.05 arcsec. The improvement in image quality is impressive, and illustrates in a dramatic way the power of LTAO.

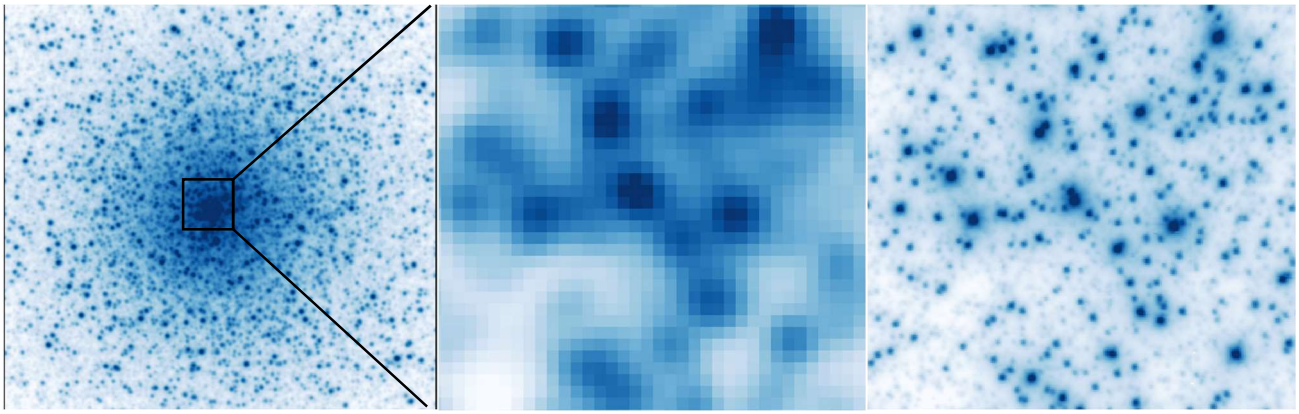

Figure 10 – Image of NGC 6388 observed with MUSE – Left: in WFM; 1arcmin x 1arcmin field of view; GLAO correction; 0.4 arcsec fwhm – Center: central part of the left image; 7arcsec x 7arcsec field of view; GLAO correction; 0.4 arcsec fwhm – Right: same area as central image; LTAO correction; 0.05 arcsec fwhm

5. CONCLUSION

Kicked-off in 2005, the AOF project is now completed. The DSM has been installed on Yepun (UT4) in December 2016 and since then is used on-sky every night for science observations (in both non-AO and AO mode). The 4LGSF is in operation since mid-2016 and has been used without any major problem so far. GRAAL has been installed on Yepun mid-2016, and GALACSI beginning of 2017. MUSE/GALACSI WFM is in operation since October 2017, HAWK-I/GRAAL since October 2018 and MUSE/GALACSI NFM since April 2019; they are all operated routinely by the Telescope and Instrument Operators in Paranal, and deliver science since then.

The GLAO mode of the AOF (GRAAL and GALACSI WFM) is behaving as expected. The delivered image quality is improved, the gain in fwhm depending only on the content of turbulence in the ground layer. An image quality as good as 0.3 arcsec fwhm can be delivered to HAWK-I by GRAAL 30% of the time, while it is almost impossible to get it otherwise. The most likely image quality delivered to MUSE by GALACSI is 0.3 arcsec, while it is only 0.6 arcsec in seeing limited mode.

The LTAO mode of GALACSI can deliver a Strehl Ratio at 650 nm better than 5% for seeing values up to 0.8 arcsec and a maximum NGS magnitude of 14. This corresponds to an image fwhm of 30 mas. In very good seeing conditions (better than 0.5 arcsec), the GALACSI LTAO delivers Strehl Ratios larger than 10% at 650 nm, with fwhm better than 20 mas.

The operation of the AOF is fully automatic, and has been optimized to reduce the overheads to less than 2 minutes. The complete system, together with the associated scientific instruments, can be operated at night by a single operator and is showing so far a reliability equivalent to other much simpler facilities on the mountain. With the advent of AOF, AO engineering entered a new era where its complexity can now be fully hidden, leaving the floor to science observations.

6. ACKNOWLEDGEMENTS

I am very grateful to all my colleagues at ESO involved in the AOF project for so many years, and more particularly to: J. Paufique, P. La Penna, E. Vernet, J.-F. Pirard, W. Hackenberg, H. Kuntschner, J. Vernet, R. Siebenmorgen, F. Selman, P. Hibon, B. Yang, G. Hau, F. Vogt, C. Opitom, M. Le Louarn, S. Stroebele, J. Kolb, S. Oberti, P. Haguenauer, D. Bonaccini Calia, T. Pfrommer, R. Holzloehner, S. Lewis, J.L. Alvarez, R. Conzelmann, R. Guzman Collazos, M. Quattri, P. Jolley, R. Ridings, J.A. Abad, C. Frank, J. Quentin, B. Delabre, S. Guisard, L. Pettazzi, S. Babak, F. Gago, M. Suarez, A. Jost, I. Guidolin, L. Kern, G. Fischer, A. Haimerl, C. Soenke, M. Downing, J. Reyes, L. Mehrgan, G. Finger, M. Kiekebusch, M. Comin, R. Donaldson, P. Duhoux, J. Argomedo, S. Tordo, J.-L. Lizon, C. Dupuy, E. Aller-Carpentier, P. Amico, P. Haguenauer, J. Valenzuela, J.-C. Guerra, C. Reyes, I. Blanchard, D. Parraguez, I. Aranda, N. Hubin, L. Pasquini, B. Leibundgut

I would like also to thank our industrial partners which made our dreams possible: Microgate and ADS, REOSC, SESO, Winlight, e2v, TOPTICA and MPBC, TNO.

Any opinions, findings, and conclusions or recommendations expressed in this publication are those of the author and do not necessarily reflect the views of the European Southern Observatory.

REFERENCES

[1] Arsenault R., et al., “Progress on the VLT Adaptive Optics Facility”, ESO Messenger No.142, p.12 (2010)
[2] Arsenault, R., et al., “ESO Adaptive Optics Facility Progress and First Laboratory Test Results”, Proc. SPIE 9148, 02 (2014)
[3] Kolb, J., et al., “Laboratory results of the AOF system testing” Proc. SPIE 9909-105 (2016)
[4] Paufique, J., et al., “GRAAL on the mountaintop”, Proc. SPIE 9909-91 (2016).
[5] Hackenberg, W. et al., “ESO 4LGSF: integration in the VLT, commissioning and on-sky results”, Proc. SPIE 9909-27 (2016)
[6] Arsenault R., et al., “The Adaptive Optics Facility: Commissioning Progress and Results”, ESO Messenger No. 168, p.8 (2017)
[7] ESO Announcement, “First Light for Largest Adaptive Optics System - VLT Unit Telescope 4 takes a key step towards being fully adaptive”, ann16078 (October 28th, 2016)
[8] ESO Press Release, “Cutting-edge Adaptive Optics Facility Sees First Light - Spectacular improvement in the sharpness of MUSE images”, eso1724 (August 2nd, 2017)
[9] Leibundgut B., et al., “MUSE WFM AO Science Verification”, ESO Messenger No. 170, p.20 (2017)
[10] Briguglio, R., et al., “The deformable secondary mirror of VLT: final electro-mechanical and optical acceptance test results”, Proc. SPIE 9148 (2014)
[11] Downing M., et al, “AO wavefront sensing detector developments at ESO”, Proc. SPIE 774204-1 (2010)
[12] Suarez Valles M., et al, « SPARTA for the VLT: status and plans”, Proc. SPIE 84472Q-2 (2012)
[13] Oberti, S., et al., “AOF laser tomography mode: reconstruction strategy and first test results”, Proc. SPIE 9909-68 (2016)
[14] Oberti, S., et al., “The AO in AOF”, Proc. SPIE 10703-53 (2018)
[15] Kiekebusch, M., et al., “Control software for the AO modules of the AOF project”, Proc. SPIE 10707-103 (2018)
[16] Kolb, J., et al., “Review of AO calibration, or how to best educate your AO system”, Proc. SPIE 9909-20 (2016)